ELSEVIER

Journal of Structural Geology 29 (2007) 100–116

JOURNAL OF STRUCTURAL GEOLOGY

www.elsevier.com/locate/jsg

Displacement transfer between intersecting regional strike-slip and extensional fault systems

V. Mouslopoulou [a,*], A. Nicol [b], T.A. Little [a], J.J. Walsh [c]

[a] *School of Earth Sciences, Victoria University of Wellington, PO Box 600, Wellington, New Zealand*
[b] *GNS Science, PO Box 30368, Lower Hutt, New Zealand*
[c] *Fault Analysis Group, University College Dublin, Dublin 4, Ireland*

Received 22 December 2005; received in revised form 12 July 2006; accepted 10 August 2006
Available online 24 October 2006

Abstract

Interaction and displacement transfer between active intersecting strike-slip (or transform) and extensional fault systems are examined. Outcrop data from a well-preserved strike-slip fault and rift intersection in New Zealand are compared to a global data set of 13 such intersections in both continental and oceanic crust. Displacement transfer between strike-slip and normal faults is typically accomplished by gradual changes of fault orientations and slip vectors close to the intersection zone. For two- and three-plate configurations, these changes result in sub-parallelism of the slip vectors of the component faults with their line of intersection. The dimensions of the area over which fault-strike and slip vectors change are principally controlled by the extent to which displacements on the dominant of the two intersecting fault systems are confined to a single slip surface or distributed across a zone. Where slip is spatially distributed, the region in which the two displacement fields are superimposed produces transtension and associated oblique slip. This distributed off-fault deformation facilitates the development of a quasi-stable configuration of the fault intersection region, maintaining both the regional geometry and kinematics of the intersection zone which, in many cases, would not be possible for rigid-block translations. The dimensions of the transition zone are larger for continental crust than for oceanic crust because oceanic crust is thinner, fault geometries in oceanic crust are simpler two-plate configurations and the slip vectors of the component intersecting fault systems are sub-parallel.

Keywords: Displacement transfer; Fault intersection; Rifting; Strike-slip faulting; Slip vectors; Triple junction; North Island Fault System; Taupo Rift; New Zealand

1. Introduction

Fault interactions are an essential feature of all fault systems and are generally accommodated either by hard-linkage, in which faults physically link, or by soft-linkage, in which displacement is transferred by distributed (i.e. ductile) deformation of the rock volume between faults. In circumstances where faults are active synchronously, interaction promotes displacement transfer and kinematic coherence within a fault system (Dahlstrom, 1969; Walsh and Watterson, 1991). Kinematic coherence (i.e. interdependence of displacement rates of all faults of the interacting fault systems) would be expected where different types of faults co-exist in close proximity and collectively accommodate regional strains imposed, for example, by plate motions. Despite its likely importance, kinematic coherence may be difficult to document using outcrop data sets which are rarely complete. In this paper we examine how kinematic coherence and associated displacement transfer are achieved between intersecting strike-slip (or transform) and extensional fault systems in the upper crust.

Fig. 1 illustrates two fundamental plate geometries for intersecting strike-slip and normal fault systems: (1) Geometries in which both normal and strike-slip faults terminate in the

* Corresponding author. Present address: Fault Analysis Group, Department of Geology, University College Dublin, Dublin 4, Ireland. Tel.: +353 1 7162611; fax: +353 1 7162607.
E-mail address: v.mouslopoulou@gns.cri.nz (V. Mouslopoulou).

0191-8141/$ - see front matter © 2006 Elsevier Ltd. All rights reserved.
doi:10.1016/j.jsg.2006.08.002

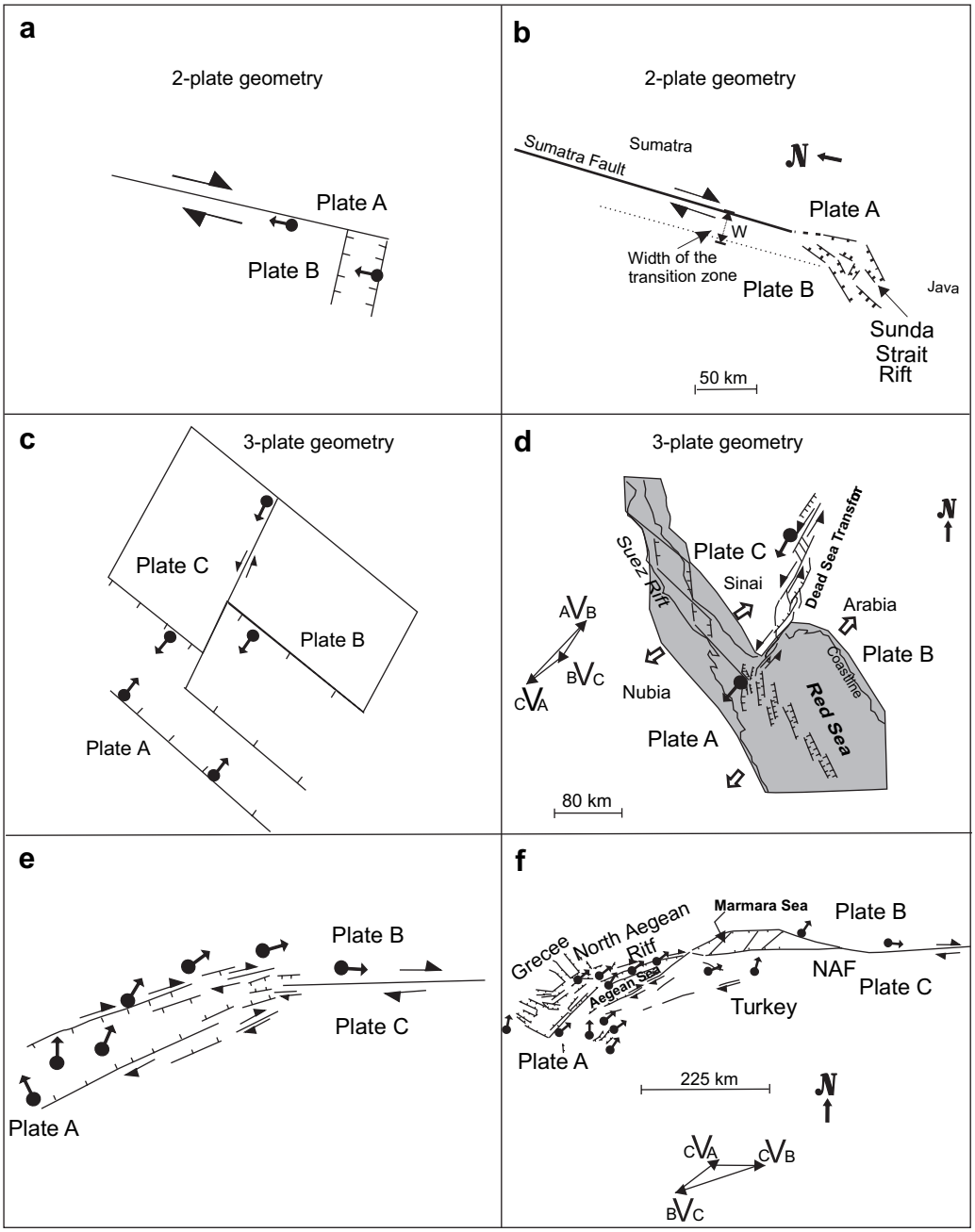

Fig. 1. (a) Displacement transfer model for a two-plate intersection assuming rigid-block translations. (b) Schematic fault map illustrating the southern termination of the Sumatra Fault against the Sunda Strait Rift. The change of strike of the normal faults at the tip of the strike-slip fault occurs within a transition zone, the width of which is shown (modified after Lelgemann et al., 2000). (c) Displacement transfer model for a three-plate configuration assuming rigid-block translations. (d) Schematic fault map of the Red Sea Rift—Dead Sea Fault—Suez Rift triple junction (modified after Courtillot et al., 1987). Large unfilled arrows show the extension direction of rifting, while the grey shaded area outlines the extent of the rift. (e) Schematic diagram illustrating displacement transfer through gradual rotation of slip vector azimuths towards parallelism across the intersection zone of the fault systems. (f) Schematic fault map of the intersection of the North Anatolian Fault (NAF) and the North Aegean Rift, Eastern Mediterranean. Slip vectors, derived from focal mechanisms across the intersection of the two fault systems (Taymaz et al., 1991), indicate the direction of motion of the north side of the faults relative to the south. Horizontal projections of slip vectors are indicated by the filled circles and attached arrows for all figures.

intersection zone, equivalent to a two-plate configuration (Fig. 1a). These two-plate geometries may occur at the tips of large strike-slip or transform faults, where strike-slip displacements are transferred into a rift, such as that which occurs between the termination of the Sumatra Fault and the Sunda Strait Rift (Fig. 1b). (2) Geometries in which one of the fault systems terminates against the other are analogous to triple junctions where the faults define three plates with summed slip azimuths across the intersection equal to zero (Fig. 1c). The Sinai triple junction in the Arabian Peninsula represents such a case (Fig. 1d).

Three-plate configurations appear to be stable in two dimensions (i.e. map-view) when the two arms of the strike-slip (or transform) fault are in alignment (T-T-R triple

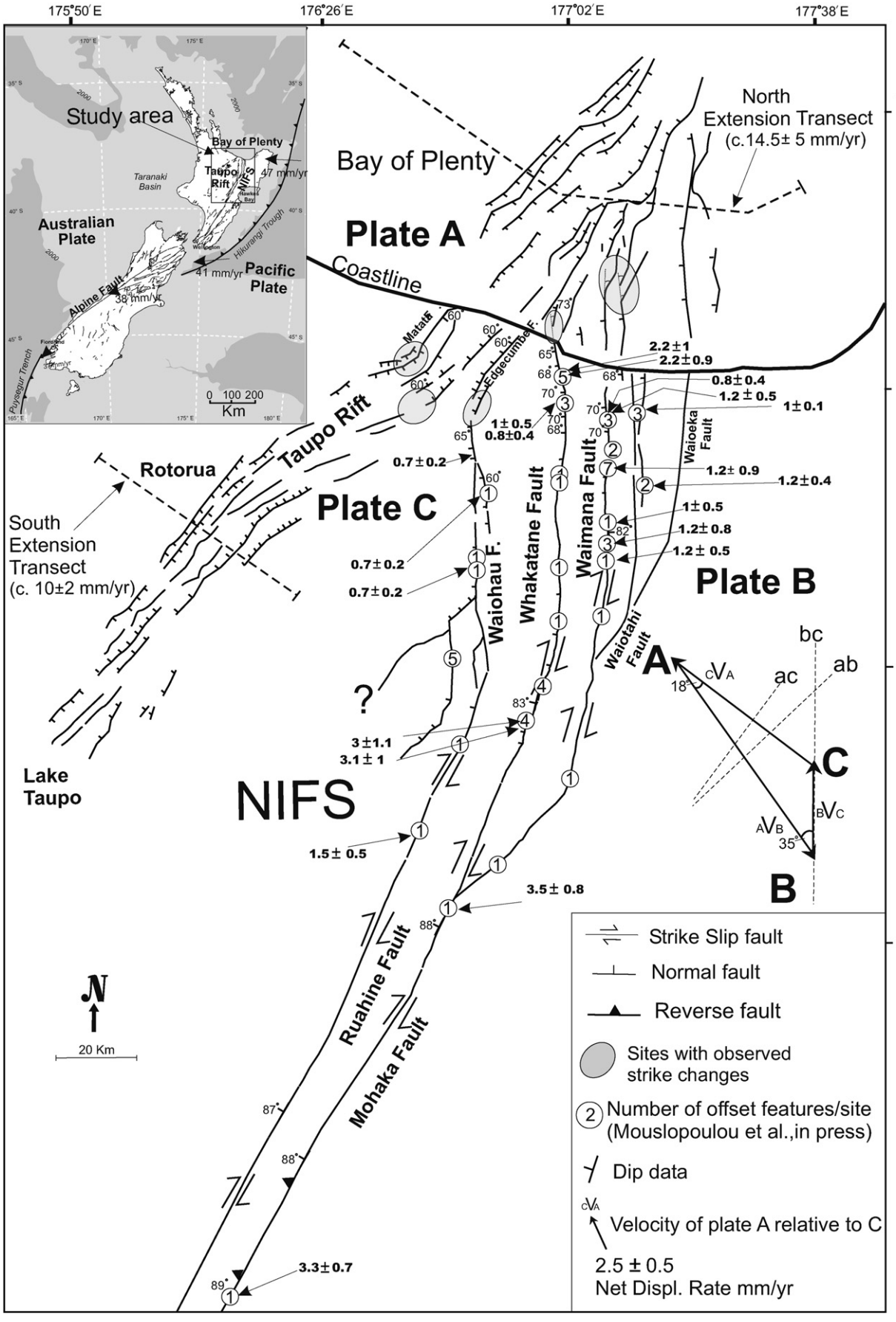
175°50′E
176°26′E
177°02′E
177°38′E
37°40′S
38°00′S
38°20′S
38°40′S
Study area
Bay of Plenty
Taupo Rift
NIFS
47 mm/yr
Taranaki Basin
Australian Plate
Pacific Plate
41 mm/yr
Hikurangi Trough
Alpine Fault
38 mm/yr
Puysegur Trench
0 100 200 Km
North Extension Transect (c.14.5± 5 mm/yr)
Plate A
Coastline
Matata F.
Edgecumbe F.
2.2±1
2.2±0.9
0.8±0.4
1.2±0.5
1±0.1
1±0.5
0.8±0.4
Waioeka Fault
Taupo Rift
Rotorua
0.7±0.2
Plate C
South Extension Transect (c. 10±2 mm/yr)
Whakatane Fault
Waimana Fault
1.2±0.9
1.2±0.4
1±0.5
1.2±0.8
1.2±0.5
Plate B
Waiohau F.
Waiotahi Fault
0.7±0.2
0.7±0.2
?
3±1.1
3.1±1
Lake Taupo
NIFS
1.5±0.5
3.5±0.8
Ruahine Fault
Mohaka Fault
3.3±0.7
N
20 Km
A
bc
ac
ab
C
B
18°
35°
Strike Slip fault
Normal fault
Reverse fault
Sites with observed strike changes
Number of offset features/site (Mouslopoulou et al.,in press)
Dip data
Velocity of plate A relative to C
2.5 ± 0.5
Net Displ. Rate mm/yr

junction) (McKenzie and Morgan, 1969) or when the two arms of the rift intersect at 90° to each other (R-R-T triple junction) (York, 1973). Under any other configuration, such a triple junction is considered to be unstable and requires temporal adjustments in the angle of fault intersection (e.g., by vertical-axis rotations) and/or changes in the velocity slip azimuths between each rigid block. For two-plate geometries, however, changes from normal to strike-slip faulting can be achieved by rigid-block translations independent of the fault intersection angle and do not necessarily require changes of slip azimuth across the intersection zone (Fig. 1a).

For three-plate geometries, the acute angle between the strikes of the intersecting fault systems can vary from 0° to 90°. For sub-perpendicular fault intersection angles, such as the intersection of the Red Sea Rift and the strike-slip Dead Sea Fault on the Arabian Peninsula (Fig. 1d), the relative slip azimuths on the intersecting strike-slip and normal faults are approximately parallel to one another, and the change in fault kinematics could be achieved by rigid-block translations with displacements confined mainly to the principal fault surfaces (Fig. 1b). For non-orthogonal intersections in which the slip vectors on the intersecting faults are not parallel, as is the case at the intersection between the North Anatolian Fault and the North Aegean Rift (Fig. 1f), displacement transfer requires rotation of the slip azimuth in the region where the faults intersect. In the upper portion of continental crust, these readjustments of slip vectors in the intersection zone must be accompanied by distributed off-fault deformation on small-scale faults (King, 1983) (Fig. 1e). Whether displacement transfer between intersecting strike-slip and normal faults (i.e. three plate geometries) is more often accommodated by rigid-block translation or by distributed deformation in the intersection zone remains unresolved.

In this paper we investigate how displacement is transferred between synchronous intersecting regional strike-slip and normal fault systems with two- or three-plate configurations. In particular, we examine how displacement is transferred between dip-slip and strike-slip faults, to what extent displacement transfer is achieved by different patterns of off-fault deformation and how the style of displacement transfer impacts on the life expectancy, and therefore stability, of the intersection zone. To answer these questions we draw on detailed data from the intersection of the strike-slip North Island Fault System (NIFS) and the Taupo Rift in onshore New Zealand and four more such intersecting strike-slip and normal fault systems in continental crust, and from nine mid-ocean ridge-transform fault intersections. The majority of these intersecting fault systems, including the New Zealand example, occur in active plate boundary zones and carry slip rates of at least 5 mm/year. Collectively, these case studies indicate the occurrence of displacement transfer between different types of faults, the propensity for slip vectors to change plunge and azimuth across the intersection zone of a two- and three-plate configuration, respectively, and the requirement for significant distributed deformation within the main fault blocks of these intersecting systems (on the scale of regional fault maps).

2. Intersecting Fault Systems

Intersecting regional strike-slip and normal faults that are presently active and moving synchronously are found globally (i.e. Joffe and Garfunkel, 1987; Taymaz et al., 1991; Mouslopoulou et al., in press). To gain a better understanding of how these intersections form and evolve we utilize three strands of data. (1) Geometric and kinematic data from the intersection of the strike-slip North Island Fault System (NIFS) and the Taupo Rift in the North Island of New Zealand (which is analogous to a triple junction), (2) published data for four examples of active intersecting strike-slip and normal faults in continental crust with two- or three-plate geometries and (3) published data for nine mid-ocean ridge-transform fault intersections.

The Taupo Rift and the NIFS in the North Island of New Zealand combine to provide an excellent example of active intersecting regional strike-slip and normal fault systems which strike at ca. 45° to each other (Fig. 2). The onshore parts of these two fault systems extend along their strikes for approximately 200 km (rift) and 450 km (NIFS). Close to their intersection, the Taupo Rift and the NIFS accommodate about 10–15 and ca. 4 mm/year of extension and right lateral strike-slip, respectively (Wallace et al., 2004; Mouslopoulou et al., in press). These fault systems are key elements of the Hikurangi margin, along which the Pacific Plate is being obliquely subducted westward beneath the Australian Plate (Fig. 2, inset). The NIFS is the principal zone of strike-slip faulting in the overriding Australian Plate. It breaks up into five main splays (i.e. Waiohau, Whakatane, Waimana, Waiotahi and Waioeka faults) approaching the northern termination where it intersects with the Taupo Rift. Within the intersection zone, the strike-slip faults of the NIFS accommodate an increasing component of normal dip-slip in a northward direction with increasing proximity to the Taupo Rift (Beanland, 1995; Mouslopoulou et al., in press), suggesting that the boundary between the two intersecting fault systems is gradational.

The transition between the rift and the strike-slip NIFS straddles the coastline, and provides one of the few active examples worldwide where elements of both intersecting fault systems are well exposed onshore (Fig. 2). In the plate tectonics nomenclature, the kinematics of this intersection is

Fig. 2. Map of the intersection of the strike-slip North Island Fault System (NIFS) and the Taupo Rift in the North Island of New Zealand. The northern tip of the NIFS comprises five main faults (Waiohau, Whakatane, Waimana, Waiotahi and Waioeka faults), whilst the Taupo Rift comprises a narrow zone of normal faults with two main rift-bounding faults (Matata and Edgecumbe faults). Dashed transects indicate locations of extension profiles across the Taupo Rift (south) and at the northern end of the intersection zone of the two fault systems (north) (see text for discussion). The three plates (A, B, C), their relative velocities ($_BV_C$, $_CV_A$, $_AV_B$) and the loci of reference frame velocities (ab, bc, ac) are indicated. The displacement rate data are from Mouslopoulou et al (in press) and the references therein. Offshore faults from Davey et al. (1995), Lamarche et al. (2000) and Taylor et al. (2004). Inset: New Zealand plate boundary setting; arrows indicate relative plate motion. The study area is located on the upper plate of the Hikurangi subduction margin.

comparable to that of a ridge-ridge-transform triple junction. Fig. 2 illustrates the three plates A, B, C comprising this configuration and presents the relative velocity circuit for these three blocks (i.e. ${}_{B}V_{C,}\ {}_{C}V_{A}$ and ${}_{A}V_{B}$) based on fault slip data (Webb and Anderson, 1998; Hurst et al., 2002; Acocella et al., 2003; Mouslopoulou et al., in press). Within the uncertainties in the data, the far-field fault slip azimuths form a closed triangle but their corresponding boundary velocities (i.e. ab, bc, and ca) do not meet at a point suggesting that this configuration is not stable in 2D (McKenzie and Morgan, 1969). The kinematics of this intersection would be stable if the two rift systems intersected at right angles (York, 1973) and/or their plate velocity vectors were parallel to one another. These requirements would be achieved if the strike of the strike-slip fault rotated to become normal to the rift (which is not the case here, Mouslopoulou et al., in press) or if slip azimuths of each fault system swing in trend to become parallel to one another.

We utilize published data from Mouslopoulou et al (in press) to explore how changes in fault orientations and late Quaternary slip vectors might be producing a quasi-stable three-plate configuration today. In detail, Mouslopoulou et al (in press) document changes in fault attitudes, displacement vectors and displacement rates on both fault systems in proximity to the intersection zone during the last 500 kyr. Ninety-seven sites were studied along the main faults in the northernmost 250 km of the NIFS and the northern 50 km of the Taupo Rift and across its intersection with the NIFS (Fig. 2). Fault attitudes (i.e. strike and dip) for both fault systems were estimated from a combination of outcrop geology, air-photo interpretation, trenching, seismic-reflection lines and gravity profiles, while slip directions are calculated from the 3D offset of various geomorphic markers (e.g. ridges, abandoned stream channels and terrace margins) and slickenside striations. Slip rates on the faults were calculated using radiocarbon dating and identification of key dated volcanic tephras on displaced landforms. Uncertainties on fault orientations and displacement rates are indicated on Figs. 2, 4 and 6b.

In addition to the New Zealand example we examine four regions of continental crust in which strike-slip and normal fault systems intersect. Three of the continental examples (i.e. the Red Sea and Dead Sea in Arabian Peninsula, the Median Tectonic Line and the Hohi Volcanic Zone in Japan and the North Anatolian Fault and the North Aegean Rift in eastern Mediterranean) provide some analogies to triple junctions, while the Sumatra case more closely resembles a simple two-plate intersection. To complement these data we also draw on a large volume of literature on the development of ridge-transform intersections in oceanic crust (Lachenbruch and Thompson, 1972; Crane, 1976; Fujita and Sleep, 1978; Choukroune et al., 1978; Fox and Gallo, 1984; Gallo et al., 1984, 1986; Goud and Karson, 1985; MacDonald et al., 1986; Pockalny et al., 1988; Taylor et al., 1994). Although oceanic crust at mid-ocean ridges is hotter, thinner and stronger than most continental crust (Kohlstedt et al., 1995), the structural evolution of ridge-transform intersections appears to be comparable to those in continental crust. Thus, while upper crustal deformation mechanisms in the intersection zones of these faults can differ between oceanic and continental crust, the kinematic requirements for displacement transfer may not. The details of each example in this worldwide database, which includes the examples presented in Fig. 1, are summarized in Table 1. These examples share many features in common with the New Zealand case but also highlight differences in the way in which upper crustal fault mosaics accommodate two- and three-plate fault junctions (e.g., Figs. 1 and 2).

In the following sections we consider in some detail how various geometrical attributes (such as fault strike, slip azimuth and fault displacement) of intersecting fault systems adjust as the zone of intersection is approached. These changes provide important constraints on how the fault systems interact and on the deformation required to achieve displacement transfer.

3. Fault intersection geometries

Intersections between strike-slip and normal fault systems in continental crust are characterised by significant variability in their geometries (Fig. 3). The strikes of the two intersecting fault systems may range from being sub-parallel to sub-perpendicular, the dominant fault system (i.e. the system not terminated at the intersection or the longer of the two fault systems) may be strike-slip or normal while the number of faults in each system may also change (two- vs. three-plate geometry). Fig. 3 excludes the situation in which neither fault system terminates at the intersection; that is, where the fault systems are entirely mutually cross-cutting because our review of the literature suggests that this four-plate geometry is rare in nature.

The New Zealand example of intersecting faults has a three-plate configuration in which rifting truncates strike-slip faulting and the component fault systems strike at about 45° to each other outside the intersection zone (Fig. 2). The strike and dip of faults in the NIFS change northwards towards its intersection with the rift. The average strike of the NIFS throughout the North Island is NNE–SSW, with the northernmost ca. 100 km of the faults striking N–S (Fig. 2). This N–S strike changes abruptly again within 5–15 km of the intersection between strike-slip faults and the main rift-bounding fault, with each of the main strike-slip faults changing clockwise in strike by up to 20–35° (Fig. 2). This abrupt change in strike may result from the "capture" of the strike-slip fault system by the NE–SW striking normal faults (outside the main rift-bounding fault) as has been observed in brittle–ductile analogue modelling (Basile and Brun, 1999). Similarly, the NE to ENE striking normal faults of the Taupo Rift change anticlockwise in strike by up to ca. 20° to a more NNE strike, as they approach the intersection with the strike-slip faults of the NIFS (Fig. 2). The net effect of these changes in the strike of the two fault systems in proximity to their mutual intersection is a reduction of the divergence of strike between the two systems from 35–45° to <10°.

These changes in fault strike occur in conjunction with a change in the dip of faults in the NIFS. To the south,

Table 1
Worldwide database presents the details of the 14 examples utilized in this study

Name	Location	Dominant fault system	Angle between fault strikes (°)[a]	Angle between far field velocity vectors(°)[b]	Horizontal Cumulative Slip Rates (mm/yr)		Width of Transition Zone (km)	Length of Transition Zone (km)	References
					Dominant	Secondary			
Taupo Rift-NIFS	New Zealand	Rift	c. 45	c. 45	10–15	4–6	45–55	60–90	1,2,3,4
NAF-Aegean Rift	Eastern Mediterranean	Strike-Slip	0–20	90–70	17–23	25–35	50–70	100–200	5,6
Red Sea Rift-Dead Sea Fault	Arabian Peninsula	Rift	65–75	20–10	7.5	6	80–120	100–140	7,8,9
Sumatra-Sunda Rift	Sumatra	Strike-Slip	40–50	50–40	6±4	<<10	c.20	40–60	10,11
MTL/Hohi VZ	Japan	Strike-Slip	35–45	55–45	<<4–9	>>1	15–25	70–80	12,13
Vema FZ / MAR	Mid-Atlantic Ridge	Oceanic Transform	88–90	2–0	24	24	9–12	9–12	14,15
Clipperton FZ / EPR	East Pacific Rise	Oceanic Transform	88–90	2–0	110	110	4–10	4–10	16
Willaumez FZ / Manus ridge	Manus Basin	Oceanic Transform	c. 70	c.20	c. 103	c. 103	5–11	10–15	17
Kane FZ / MAR	Mid-Atlantic Ridge	Oceanic Transform	84–88	6–4	30	28	5–14	5–14	18
Oceanographer FZ / MAR	Mid-Atlantic Ridge	Oceanic Transform	83–87	7–3	60	60	10–14	10–14	19
Tamayo FZ / EPR	East Pacific Rise	Oceanic Transform	88–90	2–0	60	60	4–6	4–6	20
TF-A / MAR	Mid-Atlantic Ridge	Oceanic Transform	75–80	10	c. 20	c. 20	2–4	2–4	21,22
TF-B / MAR	Mid-Atlantic Ridge	Oceanic Transform	88–90	2–0	c. 20	c. 20	6–8	6–8	21
Siqueiros FZ / EPR	East Pacific Rise	Oceanic Transform	88–90	2–0	60	60–69	5–15	5–15	23

1 = Beanland, 1995; 2 = Villamor and Berryman, 2001; 3 = Wallace et al., 2004; 4 = Mouslopoulou et al., in press; 5 = Taymaz et al., 1991; 6 = Papanikolaou et al., 2002; 7 = Joffe and Garfunkel, 1987; 8 = Picard, 1987; 9 = Moustafa, 1997; 10 = Bellier and Sébrier, 1995; 11 = Lelgemann et al., 2000; 12 = Kamata and Kodama, 1994; 13 = Tsutsumi and Okada, 1996; 14 = MacDonald et al., 1986; 15 = Van Andel et al., 1971; 16 = Gallo et al., 1986; 17 = Taylor et al., 1994; 18 = Pockalny et al., 1988; 19 = OTTER (Oceanographer Tectonic Research Team), 1984; 20 = Gallo et al., 1984; 21 = Goud and Karson, 1985; 22 = Choukroune et al., 1978; 23 = Crane, 1976. MAR = Middle Atlantic Ridge, EPR = East Pacific Rise, NIFS = North Island Fault System, NAF = North Anatolian Fault, and MTL = Median Tectonic Line.

[a] Acute angle between intersecting strike-slip and normal fault systems.

[b] Acute angle between far-field velocity vectors. Note that velocity vectors outside the intersection zone coincide with net-slip vector orientation on the principal fault surfaces on each fault system.

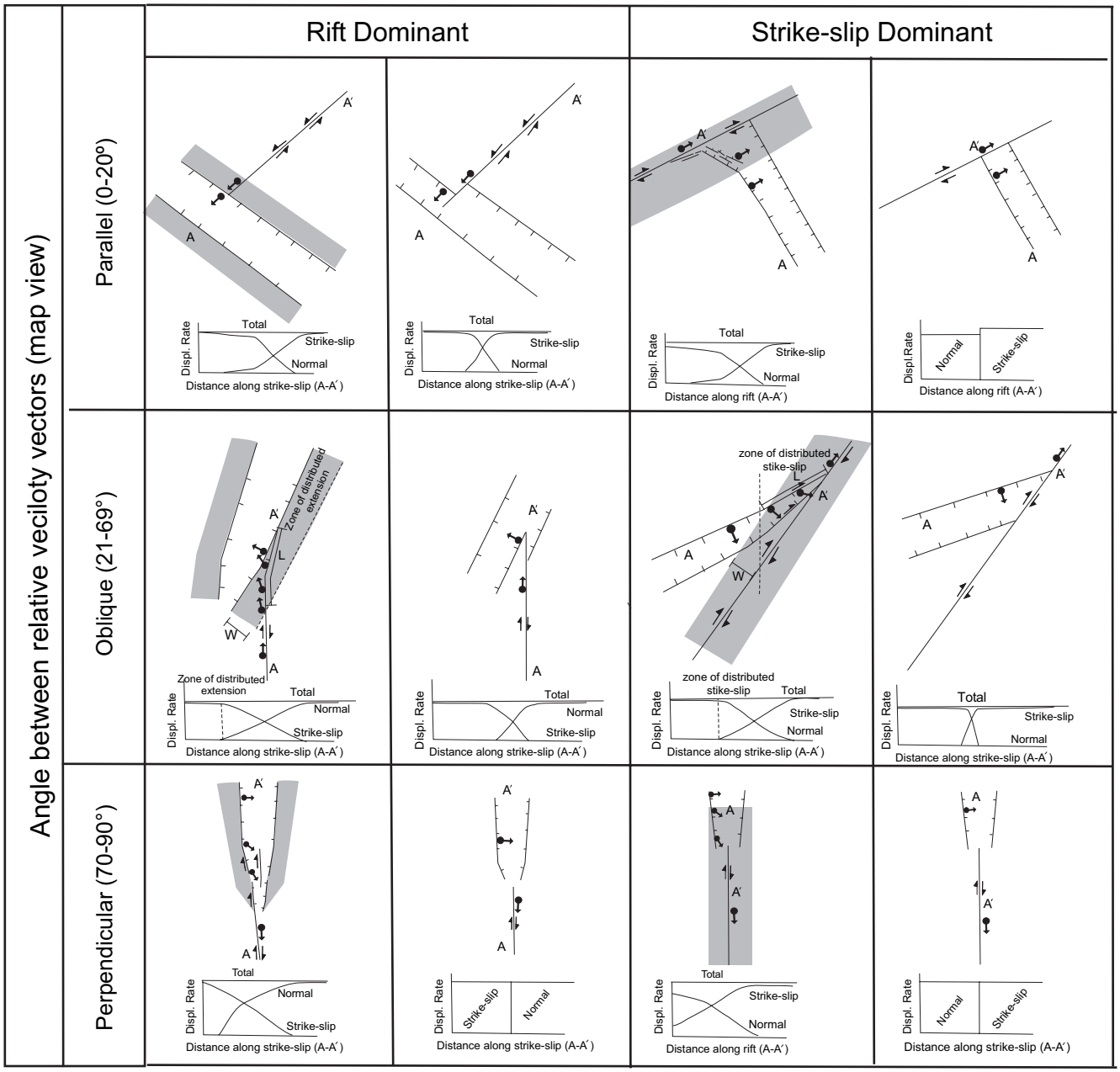

Fig. 3. Schematic diagram illustrating end-member geometries and slip vector azimuths for intersecting strike-slip and normal fault systems. In cases of three-plate geometries, the dominant fault system is the system not terminated at the intersection (i.e. through-going), whilst for the two-plate configuration it is the longer of the two fault systems. Schematic displacement profiles along the secondary fault system are indicated and permit comparison of the gradients between different intersecting geometries. Total displacement rate is uniform and conserved in its entirety across the intersection. The gradient is assumed to be equal and opposite on the component faults (these conditions may not always be met in Nature). Regions of distributed off-fault deformation are shaded grey. Horizontal projections of slip vectors are indicated by the filled circles and attached arrows.

some 120 km from the rift, the strike-slip faults at the ground surface dip steeply at 80–90° either to the east or west. These dips gradually decrease northwards towards the rift until they reach values of ca. 60–70° to the west within 10–20 km of the rift (Fig. 4). The lower dips at the northern end of the NIFS are comparable with those measured on normal faults in the upper crust and at the ground surface in the rift by seismic-reflection profiles and fault trenching (Mouslopoulou et al., in press and references therein) (Figs. 2 and 4). The observed changes of fault strikes and dips suggest a tendency for both fault systems to become sub-parallel in the proximity of their intersection. This trend is mirrored by the strike-slip fault system acquiring an increasing dip-slip component northwards towards the rift intersection (see next section for further discussion).

The changes in the geometries of intersecting faults in the New Zealand example are similar to changes in intersecting strike-slip and normal fault systems elsewhere in the world. For example, at the three-plate junction of the extensional Hohi Volcanic Zone and the strike-slip Median Tectonic Line, the strike of the secondary fault system (in this case

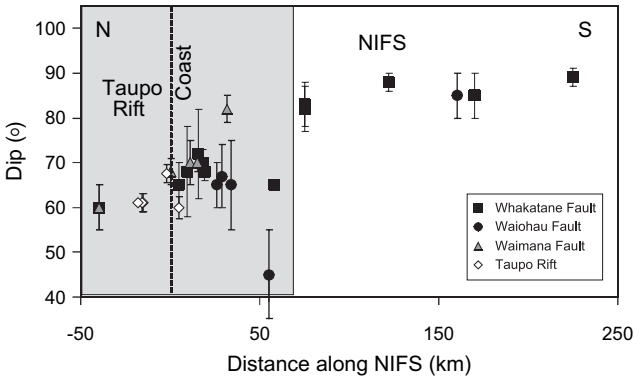

Fig. 4. Plot of measured dips for the main faults of the NIFS (Waiohau, Whakatane, Waimana) and for the main offshore faults of the Taupo Rift vs. along-strike distance measured relative to the coastline. Dip data derived from trenches, seismic-reflection and gravity profiles and outcrop geology (see Table 1 from Mouslopoulou et al., in press and the references therein). Symbols differentiate dips for each fault. Strike distance over which changes in dip of the faults are documented is shaded grey.

the rift) changes by up to 20–35° within ca. 70 km of the intersection zone to become sub-parallel to the strike-slip fault system (Fig. 5a). The Median Tectonic Line also changes strike (ca. 20°) across the intersection zone towards sub-parallelism with the faults of the rift (Fig. 5a). The change in the strike of normal faults in the Hohi Volcanic Zone within the intersection zone is consistent with a component of off-fault distributed dextral strike-slip forming up to 20 km NW of the Median Tectonic Line. Similarly, at the intersection of the strike-slip North Anatolian Fault and the North Aegean Rift (Fig. 1f), both the strike-slip fault and the rift axis change in orientation by about 20° as they approach the zone of fault system intersection (Taymaz et al., 1991; Papanikolaou et al., 2002).

In continental crust where both normal and strike-slip faults terminate at the intersection (i.e. two-plate configurations) similar strike transitions between the two fault systems have also been documented in a number of locations and settings. The southern tip of the strike-slip Sumatra Fault, for example, appears to terminate in the Sunda Strait Rift. Distal to the intersection zone, the strikes of the two fault systems differ by 40–50° (Fig. 1b) (Lelgemann et al., 2000). High resolution bathymetry data across the intersection zone reveal a change in the strike of the rift-bounding normal faults at ca. 50 km from the southern tip of the Sumatra Fault. This change in fault strike results in sub-parallelism in the attitudes of the faults within the rift and the Sumatra Fault near the intersection zone (Lelgemann et al., 2000).

The changes in the geometries of the intersecting fault systems described above are all for intersection angles of $\leq 50°$. In cases where the component fault systems are pure strike-slip and dip-slip and strike perpendicular to each other, either under a three- or two-plate configuration, their slip azimuths will be in near alignment. Because of this sub-parallelism strike-slip and normal faults intersecting at 90° can slip simultaneously without requiring significant changes in fault strike to effect the required displacement transfer. This argument is consistent with the apparent lack of change in strike of the strike-slip Dead Sea Fault as it approaches the Red Sea Rift (e.g. Figs. 1c, d and 3) but appears to be inconsistent with many ridge-transform systems in oceanic crust. In these systems, which most often strike perpendicular to each other, normal faults bounding the walls of the rift (ridge) typically change in strike by 30–90° towards the strike of the transform fault (MacDonald et al., 1986 and references therein) (Fig. 5b) resulting in sub-parallelism of the component fault systems where they intersect. Changes in strike of normal faults approaching a transform have been documented in both slow and fast spreading centers (MacDonald et al., 1986; Gallo et al., 1986; Taylor et al., 1994) and appear to be independent of displacement rates. The change in fault strikes has been inferred to result from local re-orientation of the stress trajectories through the transmission of transform-related distributed shear into the spreading center domain (Fox and Gallo, 1984; Morgan and Parmentier, 1984; Basile and Brun, 1999). The amount of curvature of each fault is thought to depend on the ratio of the rift normal to transform shear stress exerted on the rock volume that encloses the fault (Morgan and Parmentier, 1984).

4. Slip vectors

A requirement of synchronous slip on intersecting strike-slip and normal faults is that the orientations of two or more of the principal incremental strain axes must change by 90° across the intersection zone. Where strike-slip and dip-slip faults form a three-plate configuration and do not intersect at an angle of 90°, their slip vectors must be non-parallel. For these geometries to remain stable, changes in the orientations of the principal strain axes in the intersection zone must be accompanied by a change in the fault-slip vectors, which in turn requires non-rigid block (i.e. internal) deformation. In a two-plate setting, however, where the slip azimuths of each fault system are already parallel, the motions can take place through rigid-block translations across the region of fault intersection without any change in slip vector azimuth. Two- and three-plate intersections share the requirement that the slip vector must change from chiefly horizontal to chiefly dip-parallel across the zone of fault intersection. For these reasons, only the change in the plunge of slip vectors can be compared between two- and three-plate geometries.

Fig. 3 schematically illustrates a range of possible patterns of slip vector azimuths for a number of different three- and two-plate fault geometries. Slip vectors on the intersecting fault systems and outside the intersection zone may be oriented parallel (0–20°), oblique (21–69°) or perpendicular (70–90°) to one another, with displacements being accommodated on the principal slip surfaces and/or within the rock volume surrounding these fault surfaces (indicated by the grey shaded zones). As a consequence of this distributed deformation, a combination of strike-slip and normal dip-slip would be expected in the intersection zone where slip may be oblique.

In the New Zealand example, slip vectors show a gradual change in both their trend and plunge along the faults in the NIFS northwards proximal to the rift (e.g. Figs. 6a and 7).

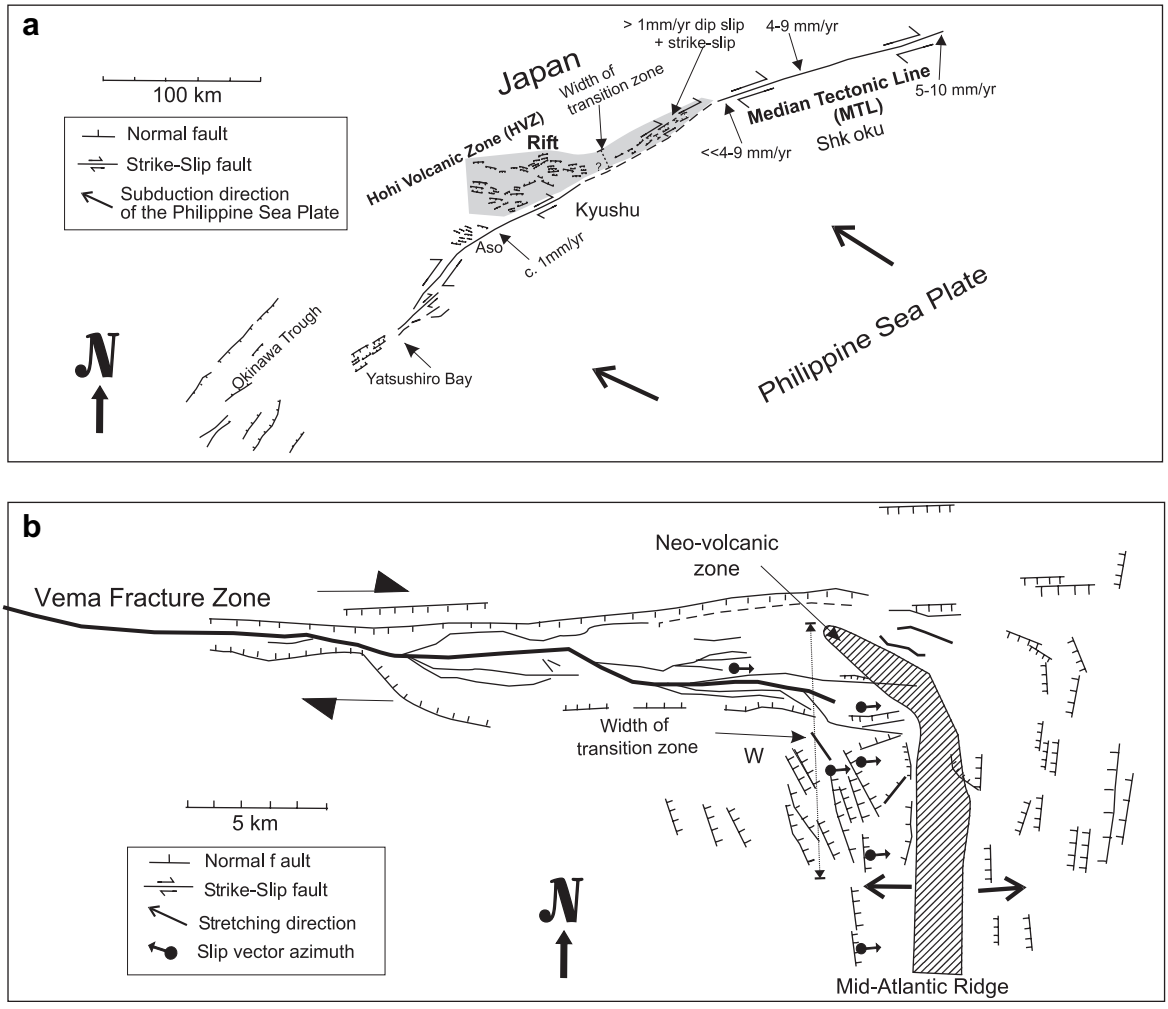

Fig. 5. (a) Intersecting strike-slip (Median Tectonic Line) and normal faults (Hohi Volcanic Zone) on Kyushu and Shikoku islands, southwest Japan (modified after Kamata and Kodama, 1994). A change in strike of the normal and strike-slip faults across the intersection zone occurs over a ca. 75 km long transition zone. Black arrows represent the subduction direction of the Philippine Sea Plate. (b) The eastern intersection of the Vema Fracture Zone with the Mid-Atlantic Ridge (modified after MacDonald et al., 1986). The change in strike of the axial normal faults, approximately 10 km from the intersection (dashed line), indicates the width (= length) of the transition zone and the associated change of their slip vector azimuths. Note that the change in the strike of the neovolcanic zone occurs much closer to the intersection than the point at which normal faults begin to change strike.

These changes accompany changes in the strike and dip of faults. On the Whakatane Fault, which is presently the fastest moving fault in the NIFS (Mouslopoulou et al., in press), slip vectors are approximately horizontal in the south (>50 km from the coast) but become progressively more dip-slip (with a pitch of ca. 55° to the northwest) close to the Bay of Plenty coastline and up to 30 km south of the main rift-bounding fault (shaded area in Fig. 6a). This gradational steepening in slip vector pitch takes place over a strike distance of approximately 60 km and is associated with a ca. 50° anticlockwise (westward) deflection in the azimuth of the slip vectors on the Whakatane Fault, a transition that could be predicted from the velocity triangle plotted in Fig. 7; that is, the CB motion is converted to a BA motion across the intersection. About 100 km to the south of Bay of Plenty coastline, there is a 25° anticlockwise change in strike of the NIFS, from NE–SW to N–S. It is interesting to note that an effect of this change is to increase the strike angle between the two fault systems, from ca. 50° to ca. 70°, and also to reduce the required change in slip azimuth across the intersection from ca. 75° to ca. 50°, correspondingly.

We also plot on Fig. 6a the plunge of the slip vector (derived from offset landform) of the Mw 6.6 1987 Edgecumbe earthquake (dashed line), which occurred on the Edgecumbe Fault, the large normal fault which bounds the eastern margin of the Taupo Rift (Beanland et al., 1989). The plunge of this earthquake slip vector is approximately parallel (i.e. within 10°) to the average plunge of the slip vectors on the northern Whakatane Fault and to the general plunge of the fault intersection (solid line intersecting the x-axis at −25 km). This sub-parallelism permits displacements to be transferred from the principal strands of the 'strike-slip' fault system to the normal faults which bound the eastern margin of the rift. The sub-parallelism of the slip vectors at the intersection of the two fault systems is consistent with the apparent absence of strike-slip offset of the southeastern margin of the rift.

The northward changes in the relative proportions of strike-slip and dip-slip along the Whakatane Fault (Fig. 6b) are

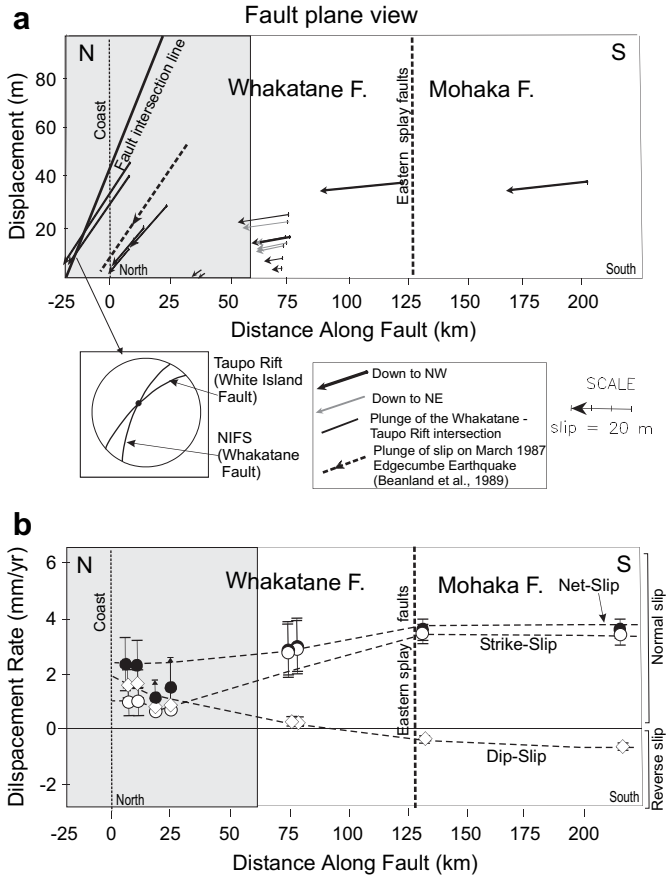

Fig. 6. (a) Fault plane view illustrating the pitch of the slip vectors along the Whakatane–Mohaka Fault. Length of arrows is proportional to the magnitude of the slip. Black arrows represent slip down to the NW, whereas grey arrows represent slip down to the NE. The plunge of the slip vector of the Mw 6.6 1987 Edgecumbe Fault (Beanland et al., 1989) earthquake is indicated (dashed line) as is the plunge of the line of intersection (thick black line) between the Edgecumbe Fault and the Whakatane Fault. (b) The three components of slip (i.e. dip-slip, strike-slip and net slip) of the Whakatane–Mohaka Fault are plotted against distance along the strike of the fault. Strike distances over which changes in the kinematics of the faults are documented are shaded grey.

accompanied by a decrease in the net-slip rate. This decrease arises in large part due to ca. 50% of its displacement being transferred onto the three other, more eastern strands of the NIFS (Fig. 2). If we take this displacement transfer into account, the net displacement rate across the NIFS may only decrease slightly from about 7.3 mm/year at the southern part of the fault system (Beanland, 1995) to about 5.5 mm/year at the coastline (Mouslopoulou et al., in press). The steepening of the slip vectors on the fault planes away from the horizontal is therefore associated with no more than a 25% loss of net slip on the principal faults in the NIFS. This loss may in part be achieved by a corresponding increase in slip on small-scale faults between the main strands of the NIFS.

The aggregation of strike-slip in the NIFS ($_{B}V_{C}$ vector) and extension in the southwestern part of the rift ($_{C}V_{A}$ vector) would be expected to result in a progressive clockwise (northeastward) swing in the extension direction in the rift from SW to NE across the intersection zone (Fig. 7). The direction of fault slip in the rift from outcrop geology (Acocella et al., 2003) and focal mechanisms (Webb and Anderson, 1998; Hurst et al., 2002) are broadly consistent and compatible with a northeastward increase in the obliquity (i.e. normal plus dextral) of fault slip in the rift. A running average of the slip azimuth for groups of five measurements suggests a ca. 20° clockwise change in slip azimuth (i.e. 325° to 345° trend). This change is accompanied by a 20° anticlockwise change in the strike of normal faults of the rift from south to north. These changes in fault kinematics in the rift combine to produce a clockwise 17° northeastward change in the trend of the extension direction (i.e. 307–324° trend) across its intersection with the NIFS. Given the uncertainties on fault-slip direction (in some cases up to ±10°), the observed changes in extension direction are consistent with the 18° predicted by summing the far-field velocity vector from the strike-slip system ($_{B}V_{C}$) with that of the rift SW of the intersection ($_{C}V_{A}$) (Fig. 7). The magnitudes of the observed and predicted changes in extension direction northward across the intersection zone with the NIFS are comparable to the 21° (i.e. 312–330° trend) predicted from modelling of GPS data (Wallace et al., 2004). The ca. 5–6° discrepancy in the trends of the modelled GPS and observed extension directions may be due to uncertainties in fault-slip directions produced by the incompleteness of both the GPS and geological data sets. Furthermore, the observed (20°) clockwise swing in the trend of the extension direction northward along the rift and across its intersection with the NIFS produces a west to east reduction in the total along-strike anticlockwise rotation of slip azimuths on faults of the NIFS (Fig. 7).

The observed changes in slip vectors across the intersection zone of the NIFS and the Taupo Rift are similar to those seen elsewhere for oblique strike-slip-rift triple junctions from the global data set. Across the intersection of the North Anatolian Fault and Aegean Rift, for example, earthquake focal mechanisms (Taymaz et al., 1991) indicate a progressive rotation of the slip vector azimuth over a strike distance of 100–200 km from strike-slip in the North Anatolian Fault to mainly normal dip-slip in the Aegean Rift (Fig. 1e). Similarly, at the intersection of the strike-slip Median Tectonic Line and the Hohi Volcanic Zone in Japan, seismic-reflection profiles from the Sea of Iyo suggest the presence of both strike-slip and dip-slip faults in the rift proximal to the Median Tectonic Line (Fig. 5a) (Tsutsumi and Okada, 1996; Kamata and Kodama, 1994). The combination of strike-slip and dip-slip in the intersection zone produces bulk transtension with summed slip vectors across the zone, intermediate in trend and in plunge between the slip vectors in the rift and on the Median Tectonic Line. Thus, the required relative velocity changes between the several mutually intersecting blocks are expressed by changes in slip vector azimuths across transition zones of finite width.

The intersection of the Red Sea Rift and the strike-slip Dead Sea Fault (Fig. 1d), is an example of a triple junction within continental crust in which the transition from strike-slip to dip-slip is achieved without apparent rotations of the slip azimuths across the intersection zone. In this special case, the slip azimuths on the intersecting strike-slip and normal faults are approximately parallel and the change in fault kinematics could

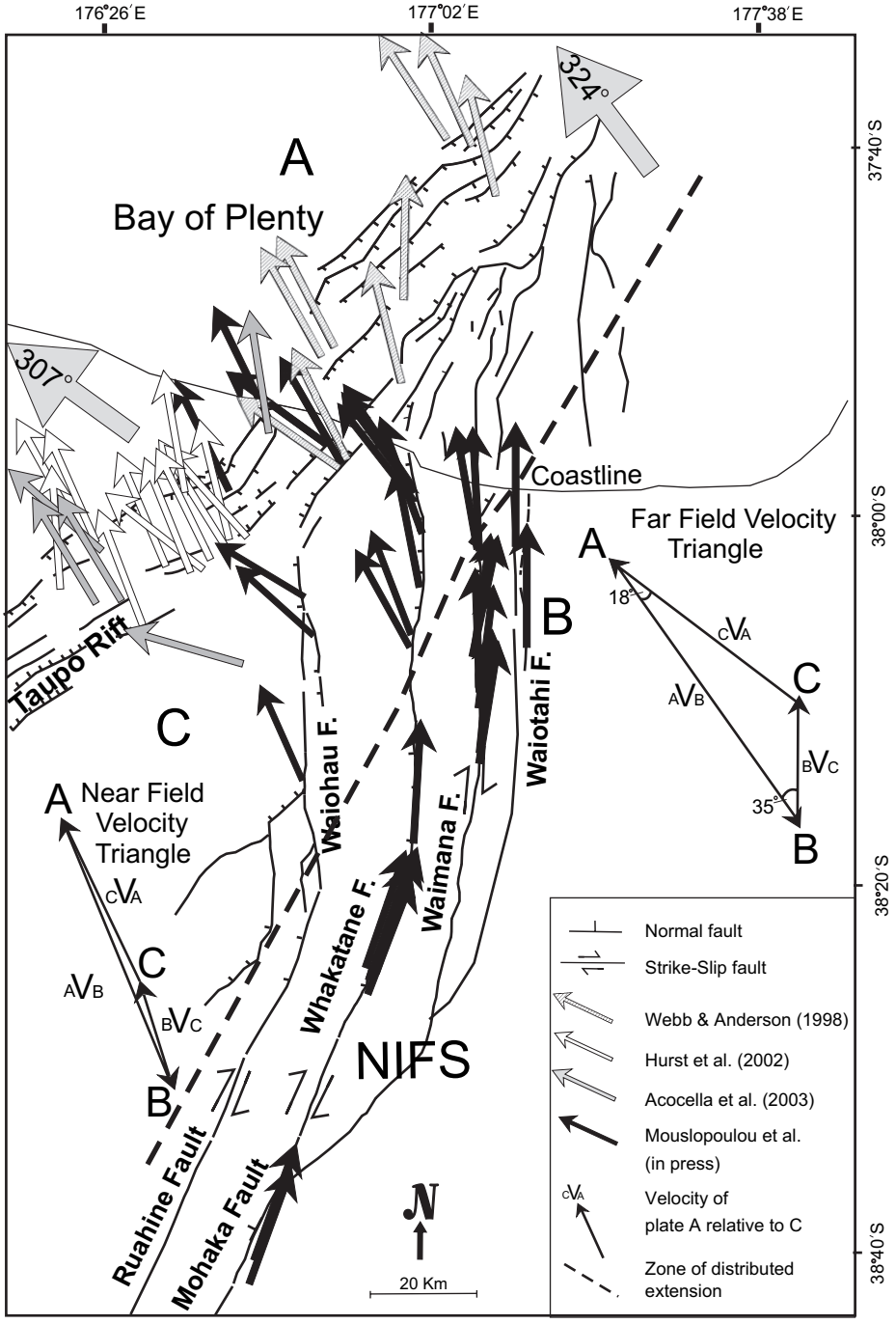

Fig. 7. Map of slip azimuths derived from outcrop geology and earthquake focal mechanisms plotted along the strike of the two fault systems and across their intersection zone. Large shaded arrows represent the average extension direction along the rift, southwest and northeast of its intersection with the NIFS, and confirm the ca. 18° predicted (using far-field velocity vectors) clockwise rotation of the extension direction across the intersection. Note the anticlockwise rotation of the slip azimuths along the NIFS. The far-field and near-field velocity triangles are indicated.

be achieved by rigid-block translations with displacements confined mainly to the principal fault surfaces (Fig. 1c). The transition from strike-slip to extension takes place mostly within the rift (i.e. in the offshore Red Sea) and up to ca. 20 km onshore and parallel to the main rift-bounding faults (Moustafa, 1997; McClay and Khalil, 1998), and as a consequence the strike-slip fault displaces the northeast margin of the rift (Fig. 1d).

Mid-ocean ridges, where strike-slip and dip-slip faults are orthogonal and slip azimuths parallel, have two-plate geometries. The geometry and kinematics of ridge-transform intersections together with finite element models of these systems indicate that the angle between the maximum horizontal tensile stress direction (σ_3) and the strike of the transform fault increases approaching the intersection (Morgan and Parmentier, 1984). Spatial changes of the maximum horizontal tensile stress direction induce local variations in the orientation of the principal strain axes and of the faults. In cases where the slip azimuths are constant across the intersection zone, changes in

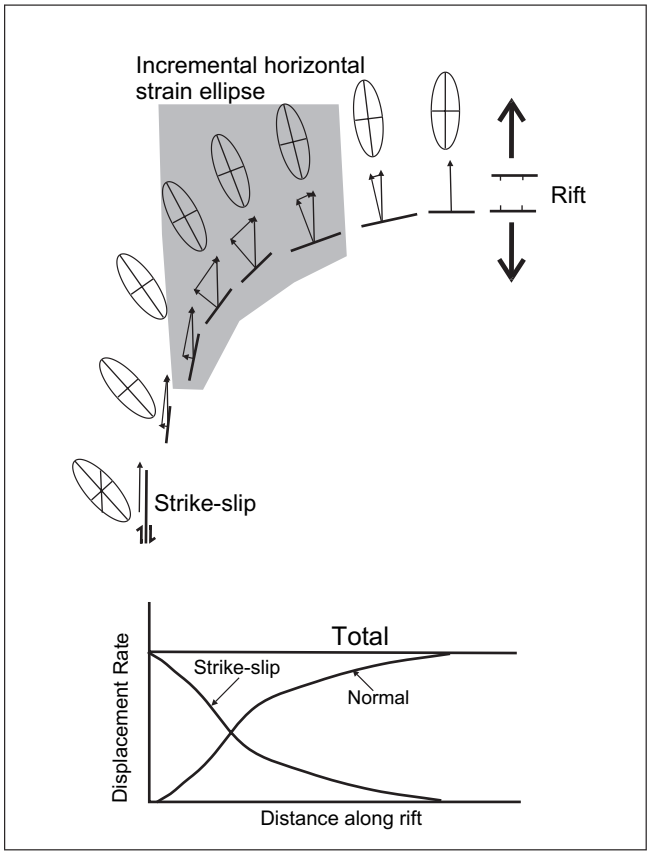

Fig. 8. Schematic diagram illustrating how the displacement transfer between orthogonal extensional and strike-slip fault systems may be achieved by rotating only the fault orientation and the individual components of slip but keeping the net-slip vector azimuth fixed. Incremental horizontal strain ellipses for each location illustrate changes in the orientations of the principal horizontal shortening and extension axes across the intersection zone. Schematic displacement profile along the rift is indicated.

fault strike result in oblique slip and associated transtension in the transition zone between the two fault systems. Such oblique slip has been inferred close to the intersection of the Siqueiros transform and the East Pacific Rise (Crane, 1976) in the 10–15 km wide intersection zone of the Manus ridge and Willaumez Transform Fault in Manus Basin (Taylor et al., 1994), and adjacent to the intersection of the Fracture Zone B and the Mid-Atlantic Ridge (Goud and Karson, 1985).

Fig. 8 schematically illustrates a transition from normal to strike-slip faulting achieved through changes of the strikes and obliquity of slip on normal faults proximal to the intersection of a ridge-transform. Oblique extension results where the two displacement fields (strike-slip and normal) are superimposed on one another. The region in which strike-slip rates dominate over normal rates is restricted to a zone immediately adjacent to the transform fault. With increasing distance from the transform, decreasing strike-slip is associated with a complementary increase in dip-slip, i.e. net slip is fixed (see displacement profiles in Fig. 8). The horizontal incremental strain ellipses for each stage of the transition illustrate changes in the orientations of the principal horizontal extension axes across the intersection zone. The transition from strike-slip to normal faulting is expected to be achieved in a similar way for two-plate junctions in continental rocks (e.g. Sumatra Fault and Sunda Strait Rift).

5. Testing and understanding displacement transfer

Displacement transfer between intersecting strike-slip and normal faults would be expected where these faults are active synchronously and is a requirement for kinematically coherent fault systems. Displacement transfer and kinematic coherence can be tested where displacement rates for the component faults can be measured immediately outside the intersection zone. At the intersection of the Red Sea Rift and the strike-slip Dead Sea Fault, for example, the 6 mm/year displacement rate of the strike-slip is equal to the decrease in extension in the rift across the intersection, from the Red Sea northwards to Gulf of Suez (i.e., 7.5–1.5 mm/year) (Joffe and Garfunkel, 1987). In the schematic displacement rate profiles of Fig. 3, total displacement rates are uniform and conserved in their entirety across the intersections. Displacement transfer observed for the Red Sea Rift–Dead Sea Fault junction and inferred in Fig. 3 has not been widely documented. In this study, however, we document the kinematic coherence of the NIFS–Taupo Rift intersection and we expect that future work will help to constrain better the existing model where displacement is transferred by non-rigid block deformation.

Displacement transfer between the NIFS and the Taupo Rift can be demonstrated with reference to the northward change in extension rates and extension directions across the rift. Extension rates across the rift to the southwest of its intersection with the NIFS are ca. 10 ± 2 mm/year in a direction approximately perpendicular to the faults (Darby et al., 2000; Villamor and Berryman, 2001; Wallace et al., 2004). North of the fault intersection rift-related extension trends at ca. 20° clockwise of the rift perpendicular direction, with rates of ca. 15 mm/year (Davey et al., 1995; Wallace et al., 2004). The ca. 5 mm/year increase in extension rates and 20° clockwise change in the slip azimuth across the intersection of the two fault systems compare favourably with the ca. 4 mm/year cumulative strike-slip displacement rates at the northern end of the NIFS (Mouslopoulou et al., in press) and with the predicted 18° clockwise rotation of the fault slip azimuths within the rift and across the intersection (Fig. 7). The similarity of these rates together with the change in the slip azimuth along the rift and across the intersection zone are consistent with the view that displacement is being transferred from the NIFS into the rift.

To test the global applicability of displacement transfer between intersecting strike-slip and dip-slip faults, we compare strike-slip[1] and extension rates on the component fault systems (Fig. 9). For two-plate geometries where both faults terminate at the intersection, strike-slip and extension are compared as close as possible to the intersection zone, whilst in cases where only one of the faults terminates (three-plate configuration), the

[1] Strike-slip rate is estimated in the extension direction (i.e. for the New Zealand example, the ca. 4 mm/year strike-slip rate on N–S striking faults result in ca. 3 mm/year rate in the NW–SE extension direction within the Taupo Rift).

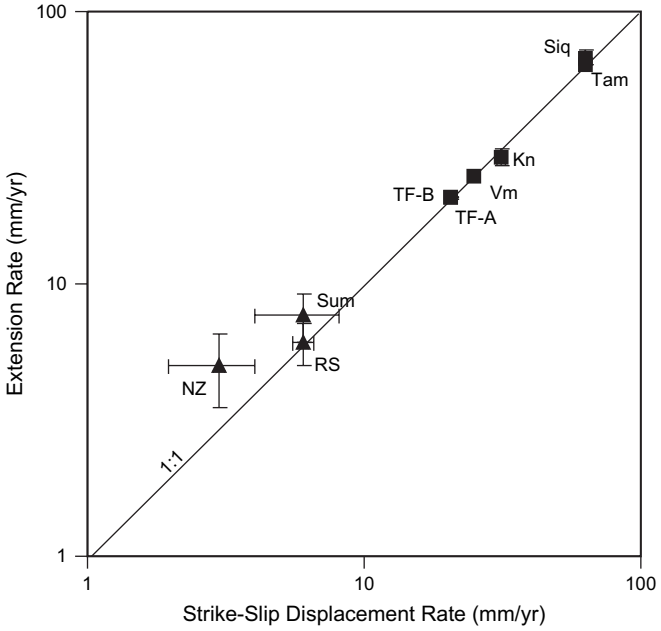

Fig. 9. Log–log plot of strike-slip and extension rates on the component fault systems of nine of the examples utilized in this study (Table 1). Note that on the *x*-axis we plot the strike-slip displacement rate which is parallel to the extension direction. Line of equal extension and strike-slip rates are indicated. Errors at a 2σ level for the New Zealand example. The error bars for the rest of the examples derived from literature. For ridge-transform intersections, errors are $\leq$0.2 mm/year (i.e. smaller than the size of the symbols). NZ = New Zealand, RS = Red Sea, Sum = Sumatra, TF-A = Transform Fault A, TF-B = Transform Fault B, Vm = Vema, Kn = Kane, Siq = Siqueiros, and Tam = Tamayo.

strike-slip or extension rates of the terminating fault are compared with the difference in strike-slip or extension across the intersection for the through-going fault. The data typically straddle the line along which strike-slip and extension are equal, supporting the suggestion that efficient displacement transfer between kinematically different fault systems is a widely occurring phenomenon. The data also suggest that the transfer of displacement between the two intersecting fault systems is principally accomplished by slip on the main mapped faults, with a relatively small component (e.g. <25%) of off-fault deformation which would be sub-resolution and could result in a rate deficit. In cases where displacement rates on the intersecting fault systems are not comparable, internal faulting within the main fault blocks (i.e. sub-parallel to the main fault strands) may constitute a significant fraction of the overall slip budget. In addition, a change in relative plate motions across the intersection and/or an inability to measure rates precisely at the margins of the intersection zone may also account for differences in the rate values across the intersection zone. In the three-plate case of the NIFS–Taupo Rift, for example, rifting is not only accommodating the horizontal translation of the NIFS but also reflects the extension induced by the southwestward oblique subduction of the Pacific Plate beneath the Australian Plate along the Hikurangi margin (Wallace et al., 2004). Therefore, the rates of extension are higher than would be expected if rifting were solely accommodating the strike-slip of the NIFS.

Determining how displacement is transferred from one fault system to another is important. Given that the transfer of displacement between two intersecting fault systems in a three-plate configuration is a three-dimensional process, we need to go beyond the 2D concept of plate tectonic stability and consider the likelihood of deforming rather than rigid plates and we also need to define the requirements for stable faulting in 3D. In 3D stable faulting across a fault junction is achieved when the trend and the plunge of the slip vector on each of the component faults are parallel with the intersection line of the two fault systems. Note that, these requirements for 3D stability, at least in theory, are not met by orthogonal R-T-T or T-R-R triple junctions which are stable in 2D, as the ca. 65° divergence in the plunge of their slip vectors at their intersection results in a kinematically unstable system.

The schematic block diagram in Fig. 10 shows the manner in which the triple junction examined in New Zealand attains a quasi-stable configuration in 3D. In the block diagram, the faults of the Taupo Rift are represented by one main marginal fault that bounds the eastern margin of the rift and accommodates most of the slip within it. The northern tips of the Waiohau, Whakatane and Waimana faults accommodate oblique extension, with the component of dip-slip gradually increasing from south to north and east to west towards the rift (Mouslopoulou et al., in press). Where the faults of the NIFS intersect the rift, their slip vectors are approximately parallel to the line of fault intersection. Therefore, the transfer of displacement between the fault systems principally takes place along their lines of intersection which, due to their sub-parallelism with the slip vectors, remain stable. As more faults of the NIFS intersect the rift, the magnitude of strike-slip and extension increase northwards along the rift.

Changes in the slip vectors along the NIFS require internal deformation in the fault blocks in between the main faults. In the hangingwalls of the faults in the NIFS (i.e. west of faults), strike-slip decreases northwards producing a net shortening in the horizontal plane which is indicated schematically in Fig. 10 by small-scale reverse faulting at high angles to the main faults. However, as this northward decrease in strike-slip is also associated with an increase in dip-slip, shortening in the horizontal plane is accompanied by extension approximately parallel to fault dip. In the footwalls of faults in the NIFS, the deformation is inverted with extension parallel to strike in the horizontal plane indicated schematically in the block diagram by small-scale normal faults formed at high angles to the main faults. This extension is accompanied by shortening approximately parallel to the dip of the fault. The magnitude of strains in fault footwalls and hanging walls cannot be determined precisely as few data are available to constrain their absolute motion during fault displacement. However, as these changes occur within an area of distributed rift-orthogonal NW–SE extension, it is more likely for normal faults to be formed at high angles to the main strike-slip faults and sub-parallel to the rift (Fig. 10). Further detailed mapping of the deforming zone between the main strands of the NIFS in combination with acquisition of earthquake focal mechanisms may help constrain better the pattern of off-fault deformation that can accommodate the observed displacement gradient on the main faults.

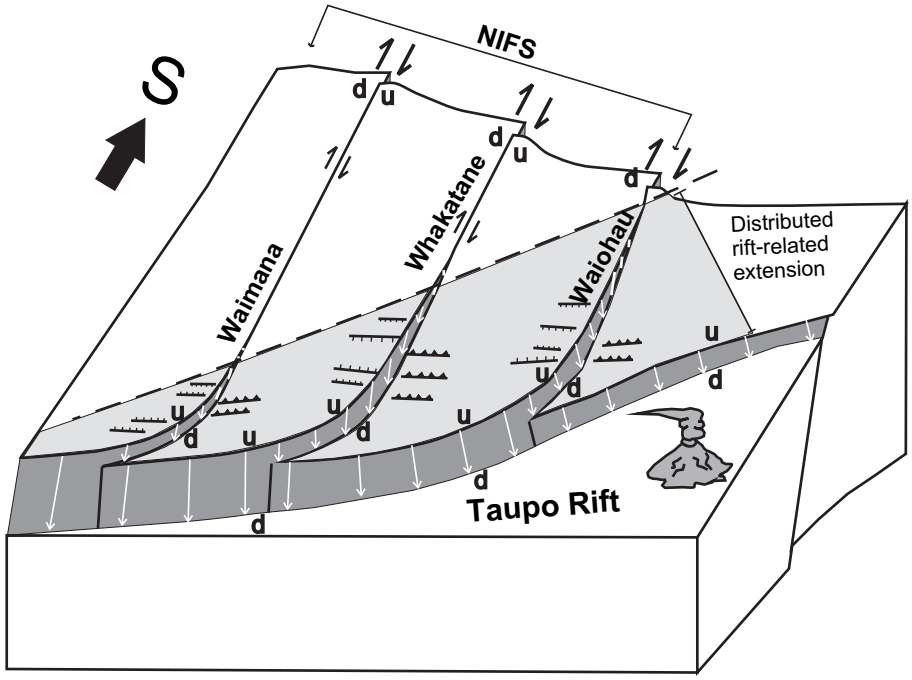

Fig. 10. Schematic block diagram showing the displacement transfer (from the strike-slip system to the normal) for the NIFS–Taupo Rift intersection, New Zealand. The block diagram summarizes the geometries and kinematics of the NIFS with increasing proximity to the Taupo Rift.

Our model of displacement transfer in the New Zealand example (Fig. 10) is consistent with available data from other three-plate fault intersections including those of the Median Tectonic Line and Hohi Volcanic Zone, and the North Anatolian Fault and Aegean Rift. In the case of two-plate configurations, such as the junction of Sumatra Fault and Sunda Strait Rift and the ridge-transform intersections, similar changes in the plunge of the slip vectors across the transition zone can be expected.

6. Dimensions and stability of intersection zone

Important questions remain as to what controls the dimensions of the transition zone from strike-slip to normal faulting. Changes of fault geometries and orientations of slip vectors on intersecting faults towards parallelism within the intersection zone occur regardless of whether the intersection consists of three (New Zealand) or two plates (ridge-transform examples), whether the rift (New Zealand) or the strike-slip fault (Japan and Sumatra examples) dominates or whether displacement rates are intermediate (ca. 5–10 mm/year) or high (ca. 100 mm/year). A common feature, however, of most intersecting strike-slip and normal fault systems that demonstrate kinematic and geometric changes proximal to the intersection zone is the presence of distributed deformation in the vicinity of the dominant fault system. The dimensions of the area over which fault geometries and slip vectors on the secondary fault change are mainly controlled by the extent to which displacement on the dominant fault system is confined to a single slip surface or distributed across a zone. Where slip on the dominant fault system is spatially distributed, the region in which the two displacement fields are superimposed will produce oblique slip and transtension (Fig. 8). The wider the zone of spatially distributed deformation associated with the dominant fault (i.e. W in Fig. 11), the longer the transition zone from one type of faulting to another (i.e. L in Fig. 11).

For the purposes of describing the dimensions of the transition zone from strike-slip to dip-slip we measure the width and the length of the transition zone. The width (W) of the transition zone is the distance, measured normal to the dominant fault and from the tip of the secondary fault, over which the deformation associated with the dominant fault is distributed. Length (L) of the transition is the distance on the secondary fault along which changes in its geometry and/or kinematics are recorded (Figs. 3 and 11). Fig. 12a, b suggests that the width (W) of the transition zone from strike-slip to dip-slip faulting and the length over which these changes are observed (L) are different for oceanic and continental examples and therefore may be influenced by crustal rheology. Deformation in oceanic crust at fault intersections more closely resembles a rigid-block process with narrower zones of deformation associated with the dominant fault (Fig. 12). This may occur because oceanic crust is thin and strong compared to continental crust (Kohlstedt et al., 1995), resulting in a relatively confined deformation zone (Dauteuil et al., 2002) and therefore rapid spatial transitions from strike-slip to dip-slip. In addition to crustal rheology, the length (L) over which the kinematics and the geometries change may relate to the angle through which the trend of the velocity vectors must rotate, with longer distances where the angles between velocity vectors are greater (Figs. 11 and 12c).[2] This relationship can be rationalized

[2] We assume that the orientations of the velocity vectors outside the intersection zone coincide with the orientation of the slip vectors on the principal fault surfaces of each fault system.

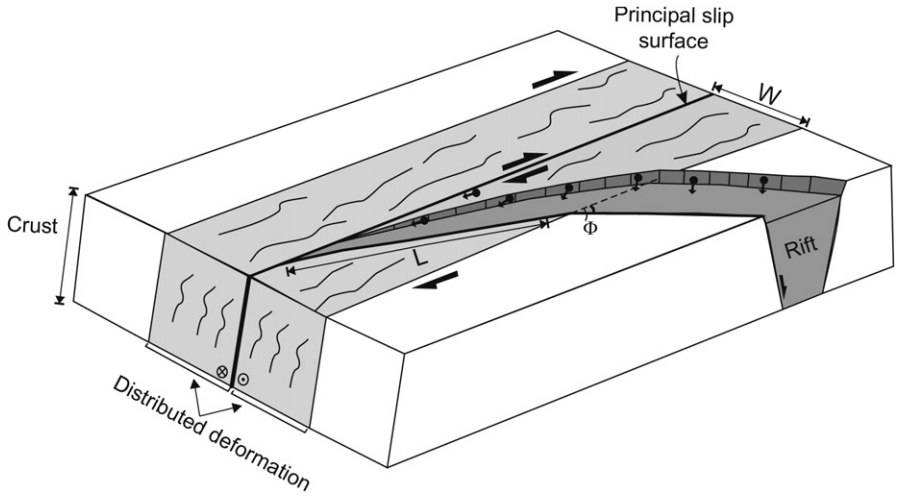

Fig. 11. Schematic block diagram illustrating the way fault geometries and kinematics of the rift change as the zone of intersection with the strike-slip fault system is approached. The smaller the angle of intersection (Φ) between the two component faults, the greater the angle through which the slip vectors of the secondary fault must change their pitch. The greater strains required for this change, however, are distributed over a longer distance (L). W = width of transition zone.

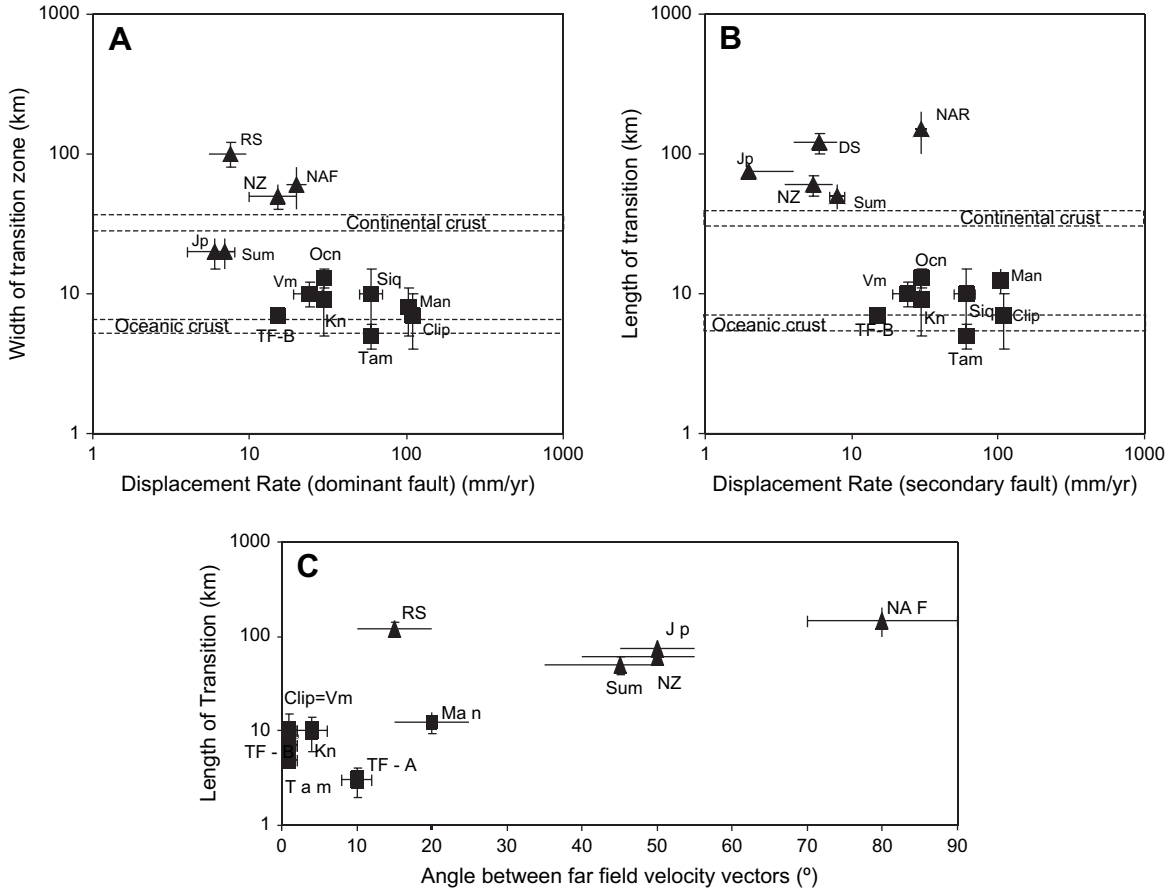

Fig. 12. (a) Log–log plot of displacement rates (on dominant faults) against the width of the transition zone for both oceanic (squares) and continental (triangles) strike-slip and normal fault intersections. (b) Log–log plot of displacement rates (on secondary faults) against the length of the transition zone for both oceanic (squares) and continental (triangles) strike-slip and normal fault intersections. (c) Semi-logarithmic plot showing a positive relationship between the length of the transition zone and the angle through which the trend of the velocity vectors rotate. Dashed lines represent average thicknesses of oceanic (6–8 km) and continental (35–40 km) crust. NZ = New Zealand, RS = Red Sea, Sum = Sumatra, NAF = North Anatolian Fault, Jp = Japan, Man - = Manus, Clip = Clipperton, Ocn = Oceanographer, TF-A = Transform Fault A, TF-B = Transform Fault B, Vm = Vema, Kn = Kane, Siq = Siqueiros, and Tam = Tamayo.

if it is considered that the greater the angle between the slip vectors of the two component systems the higher the total deformation required in the rock volume enclosing the faults. Greater displacement gradients across the intersection zone could be achieved without increasing strain magnitudes, by increasing the distance and volume over which the deformation is distributed (Fig. 11). Continental transition zones are larger than the equivalent oceanic zones due to greater thickness of the continental crust and greater complexity associated mainly with three-plate configurations which are often accompanied by greater differences between the slip vectors of the component intersecting fault systems (Fig. 12a, b).

Intriguingly, the distances over which the change in slip vector and fault strike occurs cannot be convincingly related to the displacement rates of the component faults (Fig. 12a, b). The lack of displacement rate dependency on the dimensions of the transition zone can only be quantitatively demonstrated for examples which are in all other respects similar (i.e. crustal rheology, angle between slip vectors azimuths); such constraints on the examples discussed here do not exist.

Our study has implications for the stability of strike-slip and normal fault intersections. The stability of such intersections is time and scale dependent. When one of the intersecting fault systems terminates, the fault configuration can be approximated by a triple junction with the dominant fault defining two arms of the junction. In 2D plate tectonic terms, triple junctions are assumed to develop in conjunction with rigid-block translations (McKenzie and Morgan, 1969; King, 1983; Patriat and Courtillot, 1984; Cronin, 1992) and considered to be stable if the geometry of the plates (McKenzie and Morgan, 1969) and the relative orientations of the plate boundaries (Cronin, 1992) remain constant over a finite time interval. Our study indicates, however, that rigid blocks are rarely maintained near the intersection of strike-slip and normal faults and points to a propensity for distributed deformation. The progressive changes in fault orientations and/or slip vectors and the associated distributed deformation appear to increase the stability and geological longevity of the intersection at regional scales. This point is illustrated by the NIFS and Taupo Rift intersection, which is geometrically and kinematically comparable to a ridge-ridge-transform triple junction. In formal plate tectonic terms, this type of triple junction is considered unstable (rigid blocks) (York, 1973). The intersection of the NIFS and Taupo Rift may, however, have been stable at a regional scale since 300 kyr, when throw rates on the principal faults in the NIFS and the rift increased by a factor of three (Mouslopoulou, 2006). The present fault geometries show no outward signs that strike-slip faults are displacing the rift or that the present kinematics of the active faults differ from those recorded in the last 300 kyr.

7. Conclusions

Transfer of displacement between active strike-slip and normal faults is typically facilitated by gradual changes in fault strikes, dips and slip vectors towards, and across, the intersection.

Three-plate intersections that strike at low to moderate angles to each other (up to ca. 60°) experience rotation of their slip azimuths and fault attitudes towards parallelism approaching the intersection. Two- or three-plate junctions that are orthogonal to each other, and therefore have parallel slip azimuths, appear to be characterised by gradual rotation of the plunge of slip vectors and fault attitudes on the secondary fault proximal to the intersection.

The changes in fault attitudes and slip vectors are accompanied by displacement gradients on the component faults and therefore, by distributed deformation and strain in the rock volume enclosing one or both faults over fault strike distances of up to 200 km. The distance over which these changes on the secondary (i.e. terminating) fault system are observed is defined by the width of the dominant-fault related deformation and by the angle between the far-field velocity vectors of the component fault systems across the intersection. The wider the dominant-fault related distributed deformation, the larger the area of transtensional oblique-slip arising on the secondary fault system from the superposition of the two displacement fields (i.e. dip-slip on strike-slip). Overall, the dimensions of the transition zone are larger for continental crust than for oceanic crust as the latter is thinner and comprises inherently simpler two-plate configurations which are mainly associated with narrower ranges of slip vectors between the component intersecting fault systems.

Progressive changes in the plunge and azimuth in slip vectors with proximity to fault intersections lead to a mutual parallelism of these slip vectors to the line of intersection between the two fault systems providing stable slip in 3D. This process minimizes the deformational work required for mutual slip on the two intersecting fault systems which would, otherwise, require high strains in the volume enclosing this line. Sub-parallelism of slip vectors at the fault intersection in combination with off-fault deformation increases the stability of strike-slip and normal fault intersections.

Acknowledgments

This work is the result of a PhD study undertaken at Victoria University of Wellington, New Zealand and funded by the Earthquake Commission of New Zealand, the Foundation of Research Science and Technology of New Zealand (Enterprise Scholarship) and GNS-Science. We are grateful to John Begg for beneficial reviews of this manuscript and several valuable discussions.

References

Acocella, V., Spinks, K., Cole, J., Nicol, A., 2003. Oblique back arc rifting of Taupo Volcanic Zone, New Zealand. Tectonics 22 (4), 1045.

Basile, C.A., Brun, J.P., 1999. Transtensional faulting patterns ranging from pull-apart to transform continental margins: an experimental investigation. Journal of Structural Geology 21, 23–37.

Beanland, S., Berryman, K.R., Blick, G.H., 1989. Geological investigations of the 1987 Edgecumbe earthquake. New Zealand Journal of Geology and Geophysics 32, 73–91.

Beanland, S., 1995. The North Island Dextral Fault Belt, Hikurangi subduction margin, New Zealand. PhD Thesis. Victoria University of Wellington, New Zealand.

Bellier, O., Sébrier, M., 1995. Is the slip rate variation on the Great Sumatran Fault accommodated by fore-arc stretching? Geophysical Research Letters 22 (15), 1969–1972.

Choukroune, P., Francheteau, J., Le Pichon, X., 1978. In situ structural observations along Transform Fault A in the FAMOUS area, Mid-Atlantic Ridge. Geological Society of America Bulletin 89, 1013–1029.

Courtillot, V., Armijo, R., Tapponnier, P., 1987. The Sinai triple junction revisited. Tectonophysics 141, 181–190.

Crane, K., 1976. The intersection of the Siqueiros transform fault and the East Pacific Rise. Marine Geology 21, 25–46.

Cronin, V.S., 1992. Types of kinematic stability of triple junctions. Tectonophysics 207, 287–301.

Darby, D.J., Hodgkinson, K.M., Blick, G.H., 2000. Geodetic measurement of deformation in the Taupo Volcanic Zone, New Zealand: the north Taupo network revisited. New Zealand Journal of Geology and Geophysics 43, 157–170.

Dahlstrom, C.D.A., 1969. Balanced cross sections. Canadian Journal of Earth Sciences 6, 743–757.

Dauteuil, O., Bourgeois, O., Mauduit, T., 2002. Lithosphere strength controls oceanic transform zone structure; insights from analogue models. Geophysical Journal International 150 (3), 706–714.

Davey, F.J., Henrys, S., Lodolo, E., 1995. Asymmetric rifting in a continental back-arc environment, North Island, New Zealand. Journal of Volcanology and Geothermal Research 68, 209–238.

Fox, P.J., Gallo, D.G., 1984. A tectonic model for ridge-transform-ridge plate boundaries: implications for the structure of oceanic lithosphere. Tectonophysics 104, 205–242.

Fujita, K., Sleep, N., 1978. Membrane stresses near mid-ocean ridge-transform intersections. Tectonophysics 50, 207–221.

Gallo, D.G., Kidd, W.S.F., Fox, P.J., Karson, J.A., Macdonald, K., Crane, K., Choukroune, P., Seguret, M., Moody, R., Kastens, K., 1984. Tectonics at the intersection of the East Pacific Rise with Tamayo Transform Fault. Marine Geophysical Researchers 6, 159–185.

Gallo, D.G., Fox, P.J., Macdonald, K.C.A., 1986. A sea beam investigation of the Clipperton Fracture Fault: the morphotectonic expression of a fast slipping transform boundary. Journal of Geophysical Research 91, (B3), 3455–3467.

Goud, M.R., Karson, J.A., 1985. Tectonics of the short-offset, slow-slipping transform zones in the FAMOUS area, Mid-Atlantic Ridge. Marine Geophysical Researches 7, 489–514.

Hurst, W.A., Bibby, H.M., Robinson, R.R., 2002. Earthquake focal mechanism in the Central Volcanic Zone and their relation to faulting and deformation. New Zealand Journal of Geology and Geophysics 45, 527–536.

Joffe, S., Garfunkel, Z., 1987. Plate kinematics of the circum Red Sea—a re-evaluation. Tectonophysics 141, 5–22.

Kamata, H., Kodama, K., 1994. Tectonics of an arc-arc junction: an example from Kyushu Island at the junction of the Southwest Japan Arc and the Ryuku Arca Tectonophysics 233, 69–81.

King, G., 1983. The accommodation of large strains in the upper lithosphere of the Earth and other solids by self-similar fault systems: the geometrical origin of b-value. Pure and Applied Geophysics 121, 761–815.

Kohlstedt, D.L., Evans, B., Mackwell, S.J., 1995. Strength of the lithosphere: constraints imposed by laboratory experiments. Journal of Geophysical Research 100 (B9), 17587–17602.

Lachenbruch, A.H., Thompson, G.A., 1972. Oceanic ridges and transform faults: their intersection angles and resistance to plate motion. Earth and Planetary Science Letters 15, 116–122.

Lamarche, G., Bull, J.M., Barnes, P.M., Taylor, S.K., Horgan, H., 2000. Constraining fault growth rates and fault evolution in New Zealand. EOS, Transactions, American Geophysical Union 81 (42), 481, 485, 486.

Lelgemann, H., Gutscher, M.-A., Bialas, J., Flueh, E., Weinrebe, W., Reichert, C.A., 2000. Transtentional basins in the western Sunda Strait. Geophysical Research Letters 27 (21), 3545–3548.

MacDonald, C.A.K., Castillo, D.A., Miller, S.P., Fox, P.J., Kastens, K.A., Bonnati, E., 1986. Deep-tow studies of the Vema Fracture Zone. 1. Tectonics of a major slow slipping transform fault and its intersection with the Mid-Atlantic Ridge. Journal of Geophysical Research 91 (B3), 3334–3354.

McClay, K., Khalil, S., 1998. Extensional hard linkages, eastern Gulf of Suez, Egypt. Geology 26 (6), 563–566.

McKenzie, D.P., Morgan, W.J., 1969. Evolution of triple junctions. Nature 224 (5215), 125–133.

Moustafa, A.D., 1997. Controls on the development and evolution of transfer zones: the influence of basement structure and sedimentary thickness in the Suez Rift and Red Sea. Journal of Structural Geology 19 (6), 755–768.

Morgan, J.S., Parmentier, E.M., 1984. Lithospheric stress near a ridge-transform intersection. Geophysical Research Letters 11 (2), 113–116.

Mouslopoulou, V., Nicol, A., Little, T.A., Walsh, J.J., Terminations of large strike-slip faults: an alternative model from New Zealand. In: Tectonics of Strike-Slip Restraining and Releasing Bends in Continental and Oceanic Settings. Special Volume of the Geological Society of London, in press.

Mouslopoulou, V., 2006. Quaternary geometry, kinematics and paleoearthquake history at the intersection of the strike-slip North Island Fault System and Taupo Rift, New Zealand. PhD Thesis. Victoria University of Wellington, New Zealand.

OTTER (Oceanographer Tectonic Research Team), 1984. The Geology of the Oceanographer Transform: the ridge-transform intersection. Marine Geophysical Researches 6, 109–141.

Papanikolaou, D., Alexandri, M., Nomikou, P., Ballas, D., 2002. Morphotectonic structure of the western part of the North Aegean basin based on swath bathymetry. Marine Geology 190, 465–492.

Patriat, P., Courtillot, V., 1984. On the stability of triple junctions and its relationship to its episodicity in spreading. Tectonics 3, 317–332.

Picard, L., 1987. The Elat (Aqaba)–Dead Sea–Jordan subgraben system. Tectonophysics 141, 23–32.

Pockalny, R.A., Detrick, R.S., Fox, J., 1988. Morphology and tectonics of the Kane Transform from sea beam bathymetry data. Journal of Geophysical Research 93 (B4), 3179–3193.

Taylor, S.K., Bull, J.M., Lamarche, G., Barnes, P.M., 2004. Normal fault growth and linkage in the Whakatane Graben, New Zealand, during the last 1.3 Myr. Journal of Geophysical Research 109 (B2), B02408.

Taylor, B., Crook, K., Sinton, J., 1994. Extensional transform zones and oblique spreading centers. Journal of Geophysical Research 99 (B10), 19707–19718.

Taymaz, T., Jackson, J., McKenzie, D., 1991. Active tectonics of the north and central Aegean Sea. Geophysical Journal International 106, 433–490.

Tsutsumi, H., Okada, A., 1996. Segmentation and Holocene surface rupture faulting on the Median Tectonic Line, southwest Japan. Journal of Geophysical Research 101 (B3), 5855–5871.

Van Andel, T.H., Von Herzen, R.P., Phillips, J.D., 1971. The Vema Fracture Zone and the tectonics of transverse shear zones in oceanic crustal plates. Marine Geophysical Research 1, 261–283.

Villamor, P., Berryman, K., 2001. A late Quaternary extension rate in the Taupo Volcanic Zone, New Zealand, derived from fault slip data. New Zealand Journal of Geology and Geophysics 44, 243–269.

Wallace, L.M., Beaven, J., McCaffrey, R., Darby, D., 2004. Subduction zone coupling and tectonic block rotations in the North Island, New Zealand. Journal of Geophysical Research 109 (B12), B12406.

Walsh, J.J., Watterson, J., 1991. Geometric and kinematic coherence and scale effects in normal fault systems. In: Roberts, A.M., Yielding, G., Freeman, B. (Eds.), The Geometry of Normal Faults. Geological Society of London, Special Publication No. 56, pp. 193–203.

Webb, T., Anderson, H., 1998. Focal mechanisms of large earthquakes in the North Island of New Zealand: slip partitioning at an oblique active margin. Geophysical Journal International 134, 40–86.

York, D., 1973. Evolution of triple junctions. Nature 244, 341–342.